

# Exploiting Sparsity for Long Context Inference: Million Token Contexts on Commodity GPUs

Ryan Synk<sup>\*1</sup> Monte Hoover<sup>\*1</sup>  
John Kirchenbauer<sup>1</sup> Neel Jain<sup>1</sup> Alex Stein<sup>1</sup> Manli Shu<sup>2</sup> Josue Melendez Sanchez<sup>1</sup>  
Ramani Duraiswami<sup>1</sup> Tom Goldstein<sup>1</sup>

## Abstract

There is growing demand for performing inference with hundreds of thousands of input tokens on trained transformer models. Inference at this extreme scale demands significant computational resources, hindering the application of transformers at long contexts on commodity (i.e not data center scale) hardware. To address the inference time costs associated with running self-attention based transformer language models on long contexts and enable their adoption on widely available hardware, we propose a tunable mechanism that reduces the cost of the forward pass by attending to only the most relevant tokens at every generation step using a top-k selection mechanism. We showcase the efficiency gains afforded by our method by performing inference on context windows up to 1M tokens using approximately 16GB of GPU RAM. Our experiments reveal that models are capable of handling the sparsity induced by the reduced number of keys and values. By attending to less than 2% of input tokens, we achieve over 95% of model performance on common long context benchmarks (LM-Eval, AlpacaEval, and RULER).

## 1. Introduction

Long context inference is the process by which models analyze large document collections or follow long and detailed instructions. The *context* is a series of tokens, like a set of documents or a set of files in a codebase. Increasingly, models are trained to handle larger and larger context lengths, with new models training on contexts in the millions (Liu et al., 2024b).

<sup>\*</sup>Equal contribution <sup>1</sup>University of Maryland, College Park  
<sup>2</sup>Salesforce Research. Correspondence to: Monte Hoover <mhoover4@umd.edu>, Ryan Synk <ryansynk@umd.edu>.

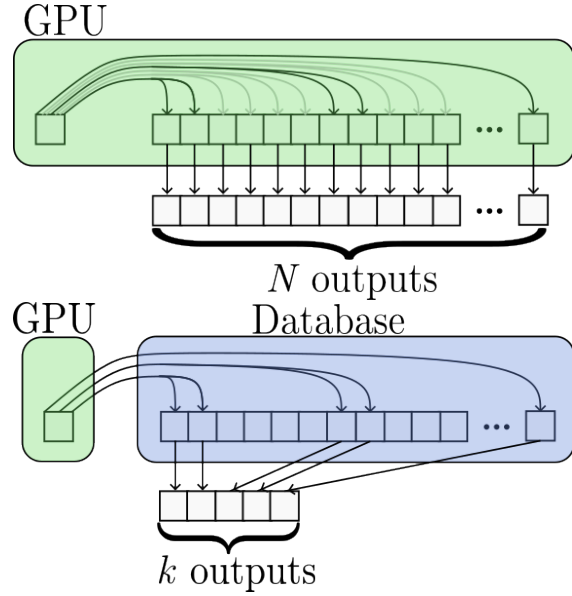


Figure 1: (top) Typical attention requires each query vector to compute an inner product with each key vector in the context window. In practice, most key vectors are insignificant to attention, so much of this computation is wasted. (left-bottom) top-k attention retrieves only the keys that contribute significantly to the attention computation, leaving the gray arrows out and achieving sublinear runtime.

Inference is done using a trained model and is divided into two steps: *prefill* and *decoding*. In the prefill stage, tokens pass forward through the model, and their key and value activations from the attention mechanism of each layer are stored in a list. This list is called the *KV cache* (Pope et al., 2023). In the decoding stage, the model uses the KV cache to generate new tokens one at a time. In a standard attention mechanism, each new token attends to every cached token in the context. When the context length is very large, both the prefill and decoding stages can become prohibitively expensive.

The prefill stage incurs an  $O(N^2)$  compute and memory cost due to the large attention matrix formed in the computation

(where  $N$  is the number of tokens in the context). To mitigate this, brute-force methods such as Ring Attention (Liu et al., 2023) have been developed. This uses round-robin communication between servers to scale computation linearly in the number of GPUs. Importantly, the prefill stage occurs only once, while the decoding stage occurs many hundreds of times.

Cache decoding incurs an  $O(N)$  compute and memory cost, as each new token must attend over all previous tokens in the context. As context lengths grow, the KV cache can become prohibitively large. To see this, note that each token in the context is embedded into a vector of size  $D$ , where  $D$  is the *hidden dimension*. The number of floating point numbers in the cache is then  $2NDL$ , where  $L$  is the number of network layers. For a value of  $D = 4096$  and  $L = 32$  as in (Grattafiori et al., 2024), at  $N = 100,000$  the memory required for the cache alone is 52GB, assuming 16 bit floating point format (Zhang et al., 2024). At this length the cache is unable to fit on most commodity GPUs.

Offloading the KV cache to the CPU can save memory, but popular offloading strategies such as (Sheng et al., 2023) move all vectors in the cache for each layer at a time. This can cause severe data movement costs, as one layer’s worth of data is 1.6GB as in our above example. These costs accumulate as decoding occurs hundreds or even thousands of times. Cache eviction methods seek to maintain a fixed cache size on the GPU by selectively removing token vectors deemed irrelevant (Zhang et al., 2023), but these strategies ultimately hurt performance as it can be difficult to tell which vectors will be needed in the future before evicting them.

We observe that modern LLMs only require the top contributing tokens to each attention computation to perform well, in line with previous work (Gupta et al., 2021). We exploit this fact to perform fast long context decoding with very little GPU memory. We build an implementation of attention in which keys and values are stored in a vector database in CPU memory. When attention is computed using a query vector at decoding time, we retrieve only the keys with the highest attention scores. This can be done in sublinear time using an approximate  $k$ -nearest neighbor search over the cache database, enabling long context inference using plentiful and cheap CPU memory, and without the heavy computational overhead required for full attention. We incur minimal data movement costs since only a fraction of the tokens ever need to be transported on the PCIe bus.

The value of  $k$  can vary across layers: some layers may need a larger  $k$  budget than others to accurately capture their attention distributions. This allows us to achieve higher accuracy for a fixed computational budget. In addition, we analyze the validity of the top- $k$  assumption through various experiments. While methods involving the restriction of the

attention mechanism to the top- $k$  attention scores have been studied, (Gupta et al., 2021; Liu et al., 2024a; Zhang et al., 2024), top- $k$  has yet to be framed in the context of resource-constrained long context decoding with approximate nearest neighbor search. Existing implementations have not been taken to the extreme scale of 1 million tokens.

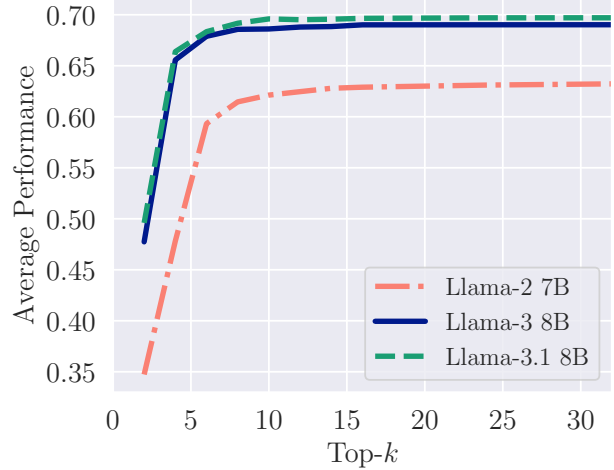


Figure 2: Performance on OpenLLM Leaderboard (Aidar Myrzakhan, 2024) using only the top- $k$  keys for each attention computation. Typical questions have a context length of  $\sim 1000$ , yet only 10 keys are needed to achieve the same performance as full attention.

Our primary contributions are summarized as follows:

- We propose a simple method for sublinear long context generation using top- $k$  attention over preprocessed states in a vector database.
- We show that this technique achieves high fidelity on common benchmarks and long-context tasks.
- We provide an empirical analysis on why top- $k$  attention works and demonstrate its effectiveness on the million token scale.
- We improve efficiency by varying the  $k$  budget on a per-layer basis.

## 2. Motivation

We observe that modern language models naturally have sparse attention patterns in which a very small number of tokens make up the vast majority of attention mass.

We visualize the sparsity of attention in Llama-3-8B using 50 Wikipedia articles in Figure 3. For the last token in each 4000-token context window, we tabulate the number of keys in the context that are needed to collect 75% of the

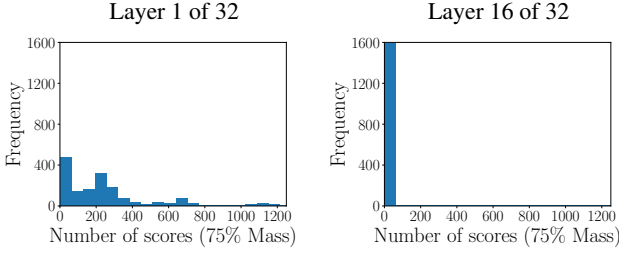


Figure 3: We analyze the number of attention scores that correspond to 75% of the probability mass for generating the next token. Each point is the number of scores of the last ‘row’ from the attention matrix required to reach 75% of the total attention. We observe each of the 32 heads across 50 samples. On the **left**, we plot the histogram for the first layer in the network, and on the **right** we plot it for layer 16.

attention mass. Only a small number of the 4000 tokens are needed to collect this mass, especially for deeper layers of the networks.

Next, we take our multi-document long context samples and ask Llama to copy one of the documents that relates to a specific topic. Figure 9 demonstrates that in expectation the attention scores (across all heads and layers) are higher for the document containing the correct document.

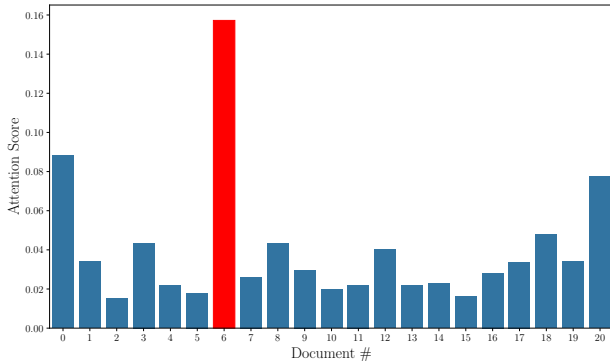


Figure 4: Where does the attention go across multiple documents? Observing all of the attention scores over all of the heads and all of the layers we see that in expectation the model is able focus most of its attention on the correct document.

To further analyze the sparsity of the model, we observe the entropy of the attention weights for each token as a function of the layer depth. Figure 5 shows that the entropy is low in all layers and decreases significantly after the first layer. Further analysis of attention sparsity across task categories and intuition on the connection between sparsity and entropy is contained in A.1.

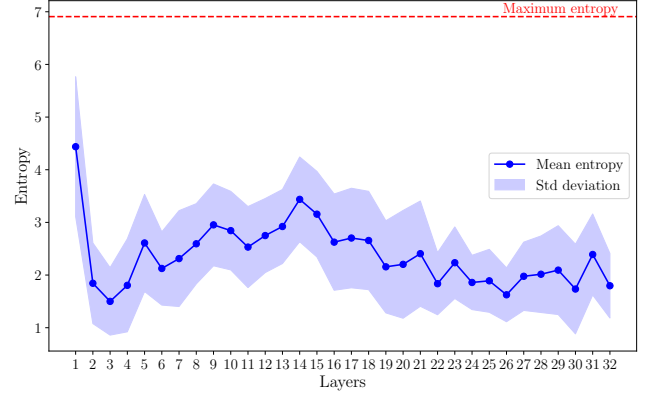


Figure 5: Entropy of the distribution of attention scores for each layer of a model, calculated as  $E = -\sum_{i=1}^N a_i \log(a_i)$ , where  $(a_1, \dots, a_N)$  is the attention score distribution. Attention score distributions are derived from 50 samples and aggregated over all heads for a given layer. Entropy serves as a measure of how concentrated the attention scores are for a given query token: low entropy indicates a large amount of attention centered over few tokens, and high entropy indicates a more uniform dispersion of attention scores.

The sparsity in Llama’s attention weights suggests that only a few key-value pairs should be needed for the model to perform close to its full capabilities. We test this hypothesis in Figure 2 by evaluating models from the Llama family across varying quantities of key-value pairs. In these experiments, we use the same number of keys for each layer of the network and average the model performance over all tasks on the OpenLLM leaderboard. We see that all three models saturate in performance by the 15th key, and the most recent (and most overtrained) variants of the model require only 10 top keys to achieve the same performance as full-scale attentions. While Figure 3 indicates that there is some spreading of the attention mass for layer 1 of the network, this tail mass seems to be unnecessary for good performance on benchmarks.

These experiments are the basis of our idea of exploiting model sparsity to speed up attention computations. Empirically, very few keys are needed to perform inference, but it is important to select keys that are primary contributors to the attention computation. To exploit this sparsity, we use a vector database to retrieve the top-k most influential tokens, enabling the GPU to perform matrix computations while the keys and values live in CPU memory. This approach alleviates both the computational and memory barriers to doing long context inference on a small GPU.

### 3. Methodology

We elaborate on our method for reducing memory costs during inference time using top-k attention. We also introduce some notation and terminology related to inference in transformers.

#### 3.1. Inference With KV Caches

As stated previously, causal inference using trained transformer models is split into two steps: the prefill and decode stages. Assume we are given a—potentially very large—set of tokens  $x$  of size  $N$  that we would like to make many queries over.

The query, key and value embeddings during prefill are of size  $(N \times D)$ , so this stage of inference incurs a maximum activation memory cost of  $O(N^2)$  due to the size of the attention matrix. Memory saving attention methods like (Dao et al., 2022) can in practice reduce this to an  $O(N)$  memory cost by tiling the attention computation. As the cache is being filled, it also grows in size and persistently costs  $O(N)$  memory across the duration of the computation.

In the decoding stage, we have a smaller query we would like to make over this context, as well as a pre-filled KV cache. Our queries comes in one token at a time, with decoding in a self-attention layer performed as follows:

$$\text{Attention}(q, K, V) = \text{Softmax}\left(\frac{qK^T}{\sqrt{D}}\right) V \quad (1)$$

Here  $q \in \mathbb{R}^{1 \times D}$  is the new query vector,  $K, V \in \mathbb{R}^{N \times D}$  are the KV cache for that layer, and  $D$  is the hidden dimension. We refer to  $S = qK^T \in \mathbb{R}^{1 \times N}$  as the *score* matrix, and the quantity  $\text{Softmax}\left(\frac{S}{\sqrt{D}}\right)$  as the *attention* matrix.

When the incoming query  $q$  is multiplied by all previous keys in the cache during decoding, the memory and compute cost incurred for the score matrix at this step is  $O(N)$ . This dependence on  $N$  for the cost of GPU memory during inference can become prohibitive for large context lengths.

#### 3.2. Top-k Attention: Accelerating Decoding

We cut down on the growing memory and compute costs by dynamically considering only the most relevant keys in the KV cache. To do this we perform a k-nearest neighbor search over the key vectors with the new query vector, returning only those value vectors corresponding to the k-largest score values.

The core of our implementation is in algorithm 1. We assume we are given a prefilled KV cache that is on the CPU. This cache is a sequence  $\{K_\ell, V_\ell\}_{\ell=1}^L$  of key and value activation tensors, one for each layer.

First we convert the key tensors across all layers in the KV cache into a nearest-neighbor search index. This index data structure can be as simple as a list (for exact nearest neighbors) or as sophisticated as a graph-based structure (for approximate nearest neighbors) as in (Malkov & Yashunin, 2020). For multi-head attention, we construct a separate index for each key head at every layer. For each layer we store the indices in a list called `K_index`.

We embed each new token during decoding into  $q$ ,  $k$ , and  $v$  on the GPU. We offload  $q$  to the CPU and perform a nearest neighbor search to get the top-k score values of the query over the context:

$$\text{vals}, I = \text{knn\_search}(q, \text{K\_index}[\ell], k)$$

Here  $k$  is the number of the largest score values we'd like use. The operation `knn_search` performs a k-nearest neighbor search of  $q$  over the key vector index for layer  $\ell$ , `K_index` $[\ell]$ . Here the k-nearest neighbor search distance is measured using the dot product metric, mirroring the attention score mechanism. This search returns two items: `vals`, a vector of size  $k$  containing the top-k score values, and  $I$ , a list of  $k$  integers mapping the score values in `vals` to their corresponding key vectors. Let  $I = (i_1, \dots, i_k)$ . We collect the relevant keys selected by the nearest neighbor search by concatenating them as row vectors together, denoted as  $V_\ell[I]$ :

$$V_\ell[I] = \begin{pmatrix} - & V_\ell[i_1] & - \\ - & V_\ell[i_2] & - \\ & \vdots & \\ - & V_\ell[i_k] & - \end{pmatrix} \in \mathbb{R}^{k \times D}$$

After the model generates the first token using the context, the key and value embeddings of this token are left on the GPU directly. This splits the total KV cache into two parts: a large part on the CPU constructed from the given context, and a small part on the GPU constructed from previously generated tokens. Given a new query, the k-nearest neighbor search is only performed on the CPU cache; on the GPU, we compute the attention directly between this query and the keys from previous generated tokens. This process resembles windowed attention (Beltagy et al., 2020a), where a window of recently generated tokens are stored directly on the GPU. These GPU window caches are labeled `K_gen` and `V_gen` in algorithm 1.

The  $V_\ell[I]$  and `vals` are then moved to the GPU. Using these, we perform the final attention computation, combining both the weighted values from the context as well as the value vectors from previously generated tokens. This method gives us a peak GPU memory cost of  $O(k)$  GPU memory cost, as opposed to  $O(N)$ . We find that  $k$  can be chosen to be a small fraction (around 1% for some tasks) of  $N$  while still recovering near-equivalent performance.

The memory savings this method allows for are highlighted in figure 10.

---

**Algorithm 1** Top-k KV Cache Decoding
 

---

**Require:** KV-Cache  $\{K_\ell, V_\ell\}_{\ell=1}^L$  where  $K_\ell, V_\ell \in \mathbb{R}^{N \times D}$ , token  $x \in \mathbb{R}^{1 \times D}$ ,  $k \in \mathbb{N}$

- 1:  $N_{gen} = 1$ ,  $K_{gen} = []$ ,  $V_{gen} = []$
- 2:  $K\_index = []$
- 3: **for**  $\ell \in \{1, \dots, L\}$  **do**
- 4:    $K\_index[\ell] \leftarrow \text{build\_index}(K_\ell)$
- 5: **end for**
- 6: **while**  $N_{gen} < N_{max}$  **do**
- 7:   **for**  $\ell \in \{1, \dots, L\}$  **do**
- 8:     Pre-attention transformer layer computations...
- 9:      $q = xW_{Q_\ell}, k = xW_{K_\ell}, v = xW_{V_\ell}$
- 10:     $K_{gen}[\ell] \leftarrow \text{concat}(K_{gen}[\ell], k)$
- 11:     $V_{gen}[\ell] \leftarrow \text{concat}(V_{gen}[\ell], v)$
- 12:     $\text{vals}, I \leftarrow \text{knn\_search}(q, K\_index[\ell], k)$
- 13:    Move  $V_\ell[I]$ ,  $\text{vals}$  to GPU
- 14:     $\hat{x} \leftarrow \text{Softmax}(\frac{1}{\sqrt{D}} \text{vals}) V_\ell[I]$
- 15:     $\hat{x} \leftarrow \hat{x} + \text{Softmax}(\frac{1}{\sqrt{D}} q \cdot K_{gen}[\ell]^T)$
- 16:    Post-attention transformer layer computations...
- 17:   **end for**
- 18:    $x \leftarrow \text{sample\_new\_token}(\hat{x})$
- 19:    $N_{gen} \leftarrow N_{gen} + 1$
- 20: **end while**

---

### 3.3. Prefilling a KV Cache at the Million Token Scale

The prefill forward pass in the construction of a KV cache potentially requires incurring the full  $O(N^2)$  memory cost. However, there are multiple ways one could prefill a cache.

Given (relatively brief) access to large amounts of compute, one could parallelize over many GPUs and construct the cache using algorithms like Ring Attention (Liu et al., 2023). The larger up-front cost of the cache construction would then be amortized over the many queries that would be made over it on much cheaper hardware. Additionally, the attention could be approximated in the construction of the cache. Algorithms like windowed attention would allow for the construction of large caches with more modest compute as in (Child et al., 2019). For small enough  $N$  (100’s of thousands of tokens), and with a high-memory GPU, the vLLM library can quickly construct KV caches by performing a standard forward pass on the model using the paged attention algorithm (Kwon et al., 2023). Finally, for very large  $N$ , top-k attention could be employed at cache construction time as well.

In our top-k experiments, we utilized flash attention and an h100 GPU to prefill the caches for our  $N=1M$  experiments. This allowed us to generate exact prefilled KV caches with

only small modifications to the network to accommodate the extreme memory requirements. We employ a chunking strategy similar to (Gupta et al., 2021). The exact modifications we made in order to prefill caches can be found in the appendix. We note that our experiments mimic an important use case of our method, namely a user with a large amount of documents that owns a limited amount of compute. In this case, the user can rent the required compute on the cloud for prefill *once*, then make as many queries as they want quickly with our method on their own hardware.

## 4. Evaluating Top-k Attention at Scale

We evaluate top-k to highlight the relationship between different values of  $k$  and performance. We find that models of various sizes and generations perform well even at small  $k$ . In general, we observe that a  $k$  equal to 1% of the total length of the context is sufficient to achieve 95% of the performance achieved with full, standard attention.

### 4.1. Evaluations

We analyze the effectiveness of the top-k attention mechanism across three benchmarks: AlpacaEval, Open LLM Leaderboard v1 tasks, and RULER. Each of these benchmark highlight a different quality of an LLM. RULER tests the model’s long context capability. AlpacaEval measures generation quality of the model. Open LLM Leaderboard v1 tasks test the model’s capabilities such as knowledge. Measuring performance across these datasets presents a comprehensive understanding of top-k.

**RULER** To demonstrate that top-k attention with small  $k$  remains effective as the context length increases, we run the RULER (Hsieh et al., 2024) benchmark suite over a series of increasing context lengths. As shown in Table 1 we run over lengths from 4k to 128k. RULER consists of thirteen total tasks from four categories. The evaluation harness runs the original Needle In A Haystack (NIAH) (Kamradt, 2023) task along with a series of more challenging variations of the task (for example, in one task the text consists entirely of labeled “needles” and the model is queries to retrieve the needle corresponding to a single label.) These NIAH tasks comprise 8 of the 13 tasks, and the remaining tasks are split into three categories: summarization proxies, multi-hop proxies, and question answering.

**AlpacaEval 2.0** We benchmark top-k attention on AlpacaEval (Dubois et al., 2024). AlpacaEval 2.0 requires a model to generate responses to 805 queries. These responses are then compared by an LLM-as-a-Judge with GPT-4 Turbo responses generated from the same query set. The winrate percentage is reported, and the LLM-as-a-Judge is GPT-4 Turbo.



Table 1: Results on RULER benchmark at various context lengths. Scores represent an average of 13 tasks in the RULER benchmark, with maximum possible score being 100. The RULER benchmark was run separately for each context length listed, and each context length was run with top-k attention for increasing values of k and also with standard, full attention.

$k$	Context Length (tokens)				
	8192	16384	32768	65536	131072
<b>2</b>	70.58	71.27	68.00	67.83	64.76
<b>8</b>	83.10	86.69	84.92	75.99	61.28
<b>32</b>	85.38	88.08	85.20	78.18	65.89
<b>128</b>	87.21	89.08	85.16	77.41	73.59
<b>512</b>	88.55	89.31	84.56	77.41	63.58
<b>2048</b>	89.42	89.31	84.53	77.33	64.62
<b>8192</b>	–	88.85	84.90	77.41	58.53
<b>16384</b>	–	–	84.81	77.26	73.40
<b>32768</b>	–	–	–	78.03	73.40
<b>Full</b>	90.31	89.45	85.03	78.87	75.17

**Open LLM Leaderboard Tasks** We investigate the performance of top-k on Open LLM Leaderboard tasks. Particularly, we evaluate different models on various values of k on the average of MMLU (Hendrycks et al., 2020), ARC tasks both easy and challenge (Clark et al., 2018), HellaSwag (Zellers et al., 2019), winogrande (Keisuke et al., 2019), OpenbookQA (Mihaylov et al., 2018), BoolQ (Clark et al., 2019), and PiQA (Bisk et al., 2020). For each task, we record the normalized accuracy when available; otherwise, we record accuracy. We report the average over tasks. We evaluate the following models on these benchmarks: Llama-1 (7B), Llama-2 (7B), Llama-3 (8B), Llama-3.1 (8B), Vicuna-v1.3 (7B), Llama-2 chat (7B), Llama-3 Instruct (8B), Llama-3.1 instruct (8B), Llama-3.2 1B instruct, and Llama-3.2 3B instruct (Touvron et al., 2023a; Zheng et al., 2023; Touvron et al., 2023b; Dubey et al., 2024; AI, 2024). The experiments are conducted using lm-eval-harness in a zero-shot setting (Gao et al., 2024).

#### 4.2. top-k is Effective at Low k

**Top-k Performance on RULER** We evaluate RULER using GradientAI’s Llama-3-8B model that has a trained context length of 262k. We find that very small values of k are sufficient to recover near-baseline performance. For every context length evaluated, 95% of the baseline performance can always be achieved with a k value of 1% or less of the total length. In Table 1, at  $k = 2$ , greater than 60% performance is achieved at all context lengths. The performance on RULER improves as k increases. Nevertheless, even at a context length of 131k tokens to achieve  $\sim 98\%$  performance of the full attention only 12.5% of the atten-

tion scores are required. This highlights the effectiveness of top-k on long context.

Interestingly, most mechanical tasks have high success rates with little variation across runs. Conversely, the question-answering tasks (from SQuAD (Rajpurkar et al., 2016) and HotpotQA (Yang et al., 2018)) end up being the tasks most indicative of model capability, with a consistently decreasing score as context length increases and as k decreases. These QA tasks were both the most revealing and had the highest variance across test runs, so allocating an extra compute budget to this subset of tasks would be helpful.

**Top-k Performance on AlpacaEval** Of the three benchmarks evaluated, AlpacaEval required the largest k as a percentage of context length to achieve 95% of baseline performance, with 2.5% of the context length being required. The trend of small k values achieving near-baseline performance was repeated across model sizes and generations.

#### Top-k Performance on OpenLLM Leaderboard Tasks

We evaluated various models to find that top-k behavior exists regardless of instruction tuning, model size, or the number of tokens the model was trained on. When comparing the models with different amounts of tokens trained, Table 6 left shows all models exhibit a similar curve with performance quickly saturating by a k value  $< 10$ , regardless of the number of tokens on which the model was trained. Furthermore, when comparing Table 6 left and center, we see that instruction models and pretrained base models exhibit the same behavior, very quickly saturating. Additionally, regardless of model size, in Table 6 right, we see that whether a model is 1B, 3B, or 8B the behavior of top-k is the same.

#### 4.3. 1M Token Generation with Top-k

To demonstrate the scaling that top-k attention permits, we use our method to generate tokens from a context window of one million tokens. We choose RULER’s Needle In A Haystack task to use for the context, and we use GradientAI’s Llama-3-8B model that has a trained context length of 1M (Gradient Team, 2024). We run this on a single-GPU node with a Faiss vector database containing the KV cache.<sup>1</sup> We also compare our method against (Xiao et al., 2023) for needle in a haystack in figure 7.

#### 4.4. Layer and Task Dependence on k

We examine the dependence of k on both tasks and also across layers of the network.

Table 3 shows how the value of k necessary to achieve

<sup>1</sup>We used a variety of k values for this experiment and it turned out that  $k=1$  is sufficient to solve Needle In A Haystack with a context length of 1 million tokens.

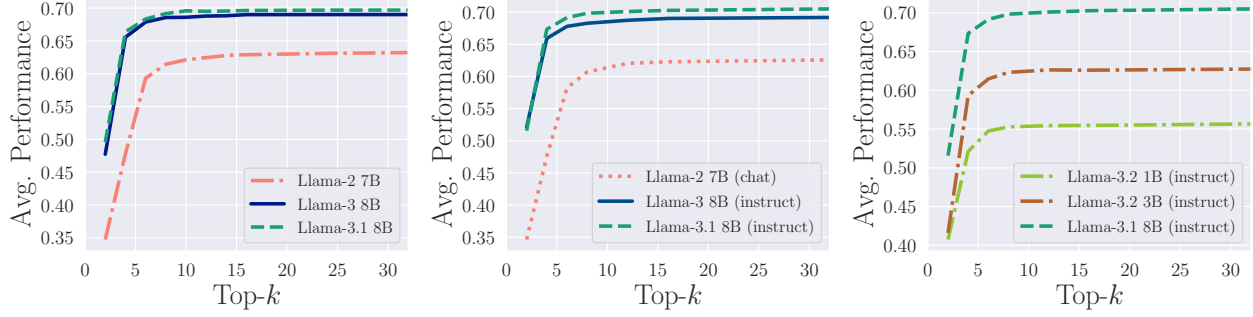


Figure 6: Top- $k$  attention is effective for OpenLLM Leaderboard Tasks even at small values of  $k$ . Left shows the average of all tasks as we increase  $k$  on pretrained base models. Center shows instruction tuned models. Right investigates the performance on different model sizes.

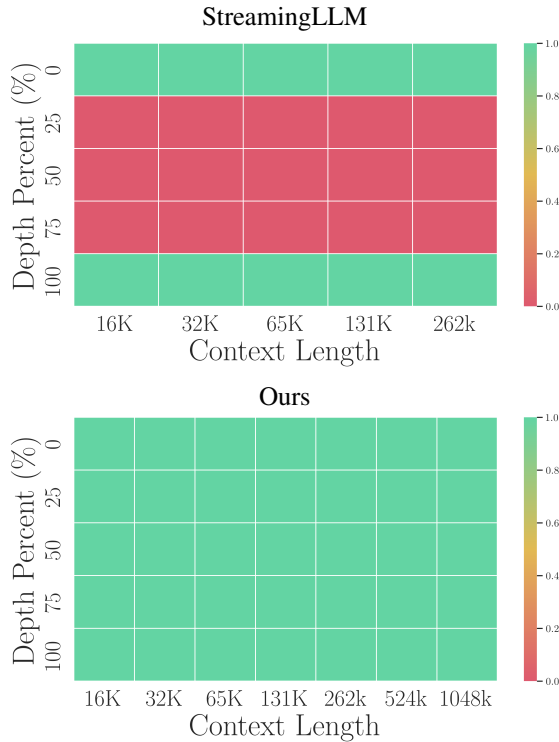


Figure 7: 1 million token needle-in-a-haystack. Comparison between the cache eviction method of (Xiao et al., 2023) and our method on a needle-in-a-haystack task. The red cells show that attention sinks are incapable of retrieving tokens outside of the local window or early sink tokens. Our method is able to do so with  $k = 10$  and extends to over 1 million tokens

Table 2: Percent of attention scores required to reach 95% of dense attention performance for different categories of tasks from the RULER benchmark.  $k$  requirements were measured by performance on contexts from 8,000-128,000 tokens. All samples from Llama3-8B.

Task Category	$k$ Required For 95% Performance
Needle In A Haystack	0.001%
Multiple NIAH	0.27%
Question Answering	0.23%
Variable Tracking	0.11%
Word Counting	8.87%

95% of base model performance varies across the tasks of RULER. For the needle in a haystack task, only a tiny fraction of the entire context is necessary to achieve 95% of the base performance of the model, whereas nearly 9% is necessary in the case of Word Counting. Most of the tasks fall under the 1% line.

We also examine the dependence of  $k$  on different layers. Recent works have shown that later layers of a transformer network tend to be less crucial to the computation than earlier ones (Gromov et al., 2024). These results motivated us to study whether the same value of  $k$  was necessary across all layers; the attention distributions of certain layers be well approximated with less  $k$  than others.

Figure 8 shows our study of  $k$  variance across layers. We vary  $k$  and plot the RULER scores as before, but we allocate  $k$  across layers in two different ways. In the uniform strategy each layer gets the same amount of  $k$ . In the adaptive strategy, we linearly increase  $k$  from the first to the last layer. At each point, the total  $k$  budget is the same: the sum across all layers of the  $k$  values used is equal. We are able to gain a non-trivial performance boost by changing our strategy of  $k$ .

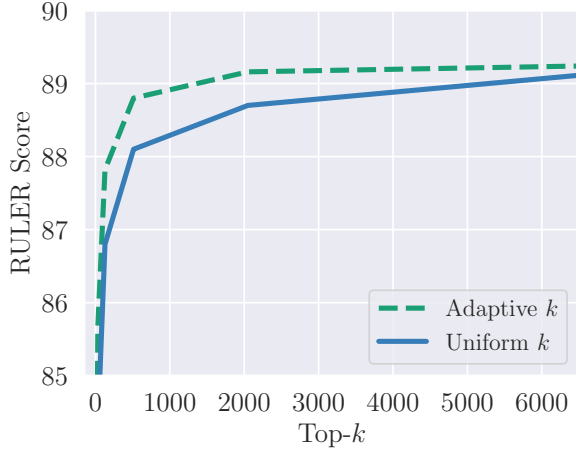


Figure 8: RULER performance of top- $k$  with a fixed vs adaptive  $k$  budget across layers. The x axis represents the total  $k$  budget, and lines are given for two  $k$  budgeting schemes: equal  $k$  across all layers and a linearly increasing  $k$  from the first to the last layer.

## 5. Related Work

The problem of making transformer model inference more efficient has been approached from many angles, and we make a brief overview of some of the relevant works below.

### 5.1. Systems Approaches

There is a long line of work in systems solutions to scale to long contexts in LLMs at inference. Flash Attention, and later Flash-Attention 2, provide theoretical linear memory complexity over the sequence length (Dao et al., 2022; Dao, 2024). vLLM’s implementation of Paged Attention (Kwon et al., 2023) optimizes for throughput over many requests, and, like Flash Attention, this Paged Attention implements a block matrix multiplication algorithm that allows for memory savings at inference time. vLLM, while very performant, does not perform any offloading and assumes the cache will be able to fit on the GPU. Liu et al. (2023) propose Ring Attention, which employs blockwise computation for the self-attention and feedforward operations, distributing long sequences over multiple devices and overlapping key-value block communication with the computation of attention. While the method is highly scalable it assumes access to datacenter-level compute. To the best of our knowledge our approach is the first to achieve inference on million token context windows on a single commodity GPU.

### 5.2. Cache Eviction Methods

A variety of methods exist for evicting tokens from the cache in order to save GPU memory. A straightforward solution is sliding window attention (Beltagy et al., 2020b),

which keeps only recent tokens of a fixed window size in the cache, and assumes that local interactions dominate. StreamingLLM (Xiao et al., 2024) discovered the “attention-sink” phenomenon and proposed a modified sliding window attention that alleviates the performance degradation in windowed attention. Both these works can fail on long contexts as important tokens in the middle of the context window may become evicted from the cache. Another widely used method is H2O (Zhang et al., 2023), a cache eviction strategy that uses information about past tokens to remove tokens from the cache. While effective in increasing decode speeds, this method is not dynamically adjustable to different queries, leading some tokens to be evicted that may be important later. Our method keeps all tokens in the cache offloaded to cheap and plentiful CPU memory, but accelerates the lookup process with fast approximate nearest neighbors.

### 5.3. Top- $k$ and Dynamic Algorithms

The closest approaches to our method in the literature are all based around the initial work on top- $k$  in Gupta et al. (2021). This method computes all scores directly before filtering out the top- $k$ , incurring quadratic computation and demanding the entire KV cache fits on GPU memory. Chen et al. (2024) also accelerate decoding by selecting relevant tokens, but take an approach based on sampling attention distributions. Singhanian et al. (2024) construct a low-cost proxy to full attention using PCA, which informs the token subset for the attention computation. However, these solutions do not support context lengths past a few hundred thousand.

Tang et al. (2024) dynamically select relevant tokens from the cache during decoding, but their method relies on a heuristic approximation of top- $k$  divided over cache pages, whereas our method utilizes a nearest-neighbor data structure. The concurrent works of (Liu et al., 2024a) and (Zhang et al., 2024) bear a resemblance to our method but enforce exactly which kind of nearest-neighbor search algorithm is employed: a custom database in the first and the method of PQ quantization in the second. Our method both generalizes their method to allow for any database and is extended to 1 million length contexts and beyond.

## 6. Conclusion

We have demonstrated the capability of a top- $k$  attention mechanism to operate at the million token scale on a single GPU. In addition, our investigation of attention distributions across layers points to future directions where the choice of  $k$  can be adapted across layers. We achieve sublinear complexity and evaluate at over 95% accuracy on common benchmarks while using only 1% of the context length on average in the attention block. This exploitation of attention sparsity opens up new directions for efficient and viable solutions to long context inference in language models.



## References

- AI, M. Llama 3.2: Revolutionizing edge ai and vision with open, customizable models. <https://ai.meta.com/blog/llama-3-2-connect-2024-vision-edge-mobile-devices/>, 2024. Accessed: 2024-10-01.
- Aidar Myrzakhan, Sondos Mahmoud Bsharat, Z. S. Open-llm-leaderboard: From multi-choice to open-style questions for llms evaluation, benchmark, and arena. *arXiv preprint arXiv:2406.07545*, 2024.
- Beltagy, I., Peters, M. E., and Cohan, A. Longformer: The long-document transformer. *arXiv:2004.05150*, 2020a.
- Beltagy, I., Peters, M. E., and Cohan, A. Longformer: The long-document transformer. *CoRR*, abs/2004.05150, 2020b.
- Bisk, Y., Zellers, R., Bras, R. L., Gao, J., and Choi, Y. Piqa: Reasoning about physical commonsense in natural language. In *Thirty-Fourth AAAI Conference on Artificial Intelligence*, 2020.
- Chen, Z., Sadhukhan, R., Ye, Z., Zhou, Y., Zhang, J., Nolte, N., Tian, Y., Douze, M., Bottou, L., Jia, Z., and Chen, B. Magicpig: Lsh sampling for efficient llm generation, 2024. URL <https://arxiv.org/abs/2410.16179>.
- Child, R., Gray, S., Radford, A., and Sutskever, I. Generating long sequences with sparse transformers, 2019. URL <https://arxiv.org/abs/1904.10509>.
- Clark, C., Lee, K., Chang, M.-W., Kwiatkowski, T., Collins, M., and Toutanova, K. Boolq: Exploring the surprising difficulty of natural yes/no questions. In *Proceedings of the 2019 Conference of the North American Chapter of the Association for Computational Linguistics: Human Language Technologies, Volume 1 (Long and Short Papers)*, pp. 2924–2936, 2019.
- Clark, P., Cowhey, I., Etzioni, O., Khot, T., Sabharwal, A., Schoenick, C., and Tafjord, O. Think you have solved question answering? try arc, the ai2 reasoning challenge. *arXiv preprint arXiv:1803.05457*, 2018.
- Dao, T. Flashattention-2: Faster attention with better parallelism and work partitioning. In *The Twelfth International Conference on Learning Representations*, 2024. URL <https://openreview.net/forum?id=mZn2Xyh9Ec>.
- Dao, T., Fu, D. Y., Ermon, S., Rudra, A., and Ré, C. Flashattention: Fast and memory-efficient exact attention with io-awareness, 2022. URL <https://arxiv.org/abs/2205.14135>.
- Dubey, A., Jauhri, A., Pandey, A., Kadian, A., Al-Dahle, A., Letman, A., Mathur, A., Schelten, A., Yang, A., Fan, A., et al. The llama 3 herd of models. *arXiv preprint arXiv:2407.21783*, 2024.
- Dubois, Y., Galambosi, B., Liang, P., and Hashimoto, T. B. Length-controlled alpacaEval: A simple way to debias automatic evaluators. *arXiv preprint arXiv:2404.04475*, 2024.
- Gao, L., Tow, J., Abbasi, B., Biderman, S., Black, S., DiPofi, A., Foster, C., Golding, L., Hsu, J., Le Noac’h, A., Li, H., McDonnell, K., Muennighoff, N., Ociepa, C., Phang, J., Reynolds, L., Schoelkopf, H., Skowron, A., Sutawika, L., Tang, E., Thite, A., Wang, B., Wang, K., and Zou, A. A framework for few-shot language model evaluation, 07 2024. URL <https://zenodo.org/records/12608602>.
- Gradient Team. Scaling rotational embeddings for long-context language models. <https://gradient.ai/blog/scaling-rotational-embeddings-for-long-context-language-models>, May 2024. Accessed: 2024-10-01.
- Grattafiori, A. et al. The llama 3 herd of models, 2024. URL <https://arxiv.org/abs/2407.21783>.
- Gromov, A., Tirumala, K., Shapourian, H., Gloriosio, P., and Roberts, D. A. The unreasonable ineffectiveness of the deeper layers, 2024. URL <https://arxiv.org/abs/2403.17887>.
- Gupta, A., Dar, G., Goodman, S., Ciprut, D., and Berant, J. Memory-efficient Transformers via Top-k Attention. In *Proceedings of the Second Workshop on Simple and Efficient Natural Language Processing*, pp. 39–52, Virtual, 2021. Association for Computational Linguistics. doi: 10.18653/v1/2021.sustainlp-1.5.
- Hendrycks, D., Burns, C., Basart, S., Zou, A., Mazeika, M., Song, D., and Steinhardt, J. Measuring massive multitask language understanding. In *International Conference on Learning Representations*, 2020.
- Hsieh, C.-P., Sun, S., Krizan, S., Acharya, S., Rekesh, D., Jia, F., Zhang, Y., and Ginsburg, B. RULER: What’s the Real Context Size of Your Long-Context Language Models?, April 2024.
- Kamradt, G. Needle in a haystack - pressure testing llms. <https://github.com/gkamradt/LLMTest>, 2023. GitHub repository.
- Keisuke, S., Ronan, L. B., Chandra, B., and Yejin, C. Winogrande: An adversarial winograd schema challenge at scale. 2019.

- Kwon, W., Li, Z., Zhuang, S., Sheng, Y., Zheng, L., Yu, C. H., Gonzalez, J. E., Zhang, H., and Stoica, I. Efficient memory management for large language model serving with pagedattention. In *Proceedings of the ACM SIGOPS 29th Symposium on Operating Systems Principles*, 2023.
- Liu, D., Chen, M., Lu, B., Jiang, H., Han, Z., Zhang, Q., Chen, Q., Zhang, C., Ding, B., Zhang, K., Chen, C., Yang, F., Yang, Y., and Qiu, L. Retrievalattention: Accelerating long-context llm inference via vector retrieval, 2024a. URL <https://arxiv.org/abs/2409.10516>.
- Liu, H., Zaharia, M., and Abbeel, P. Ring attention with blockwise transformers for near-infinite context, 2023. URL <https://arxiv.org/abs/2310.01889>.
- Liu, H., Yan, W., Zaharia, M., and Abbeel, P. World model on million-length video and language with blockwise ringattention, 2024b. URL <https://arxiv.org/abs/2402.08268>.
- Malkov, Y. A. and Yashunin, D. A. Efficient and robust approximate nearest neighbor search using hierarchical navigable small world graphs. *IEEE Trans. Pattern Anal. Mach. Intell.*, 42(4):824–836, April 2020. ISSN 0162-8828. doi: 10.1109/TPAMI.2018.2889473. URL <https://doi.org/10.1109/TPAMI.2018.2889473>.
- Mihaylov, T., Clark, P., Khot, T., and Sabharwal, A. Can a suit of armor conduct electricity? a new dataset for open book question answering. In *EMNLP*, 2018.
- Pope, R., Douglas, S., Chowdhery, A., Devlin, J., Bradbury, J., Heek, J., Xiao, K., Agrawal, S., and Dean, J. Efficiently scaling transformer inference. *Proceedings of Machine Learning and Systems*, 5:606–624, 2023.
- Rajpurkar, P., Zhang, J., Lopyrev, K., and Liang, P. Squad: 100,000+ questions for machine comprehension of text, 2016. URL <https://arxiv.org/abs/1606.05250>.
- Sheng, Y., Zheng, L., Yuan, B., Li, Z., Ryabinin, M., Chen, B., Liang, P., Ré, C., Stoica, I., and Zhang, C. Flexgen: high-throughput generative inference of large language models with a single gpu. In *Proceedings of the 40th International Conference on Machine Learning, ICML’23*. JMLR.org, 2023.
- Singhania, P., Singh, S., He, S., Feizi, S., and Bhatele, A. Loki: Low-rank keys for efficient sparse attention, 2024. URL <https://arxiv.org/abs/2406.02542>.
- Tang, J., Zhao, Y., Zhu, K., Xiao, G., Kasikci, B., and Han, S. Quest: Query-aware sparsity for efficient long-context llm inference, 2024. URL <https://arxiv.org/abs/2406.10774>.
- Touvron, H., Lavril, T., Izacard, G., Martinet, X., Lachaux, M.-A., Lacroix, T., Rozière, B., Goyal, N., Hambro, E., Azhar, F., et al. Llama: Open and efficient foundation language models. *arXiv preprint arXiv:2302.13971*, 2023a.
- Touvron, H., Martin, L., Stone, K., Albert, P., Almahairi, A., Babaei, Y., Bashlykov, N., Batra, S., Bhargava, P., Bhosale, S., et al. Llama 2: Open foundation and fine-tuned chat models. *arXiv preprint arXiv:2307.09288*, 2023b.
- Xiao, G., Tian, Y., Chen, B., Han, S., and Lewis, M. Efficient streaming language models with attention sinks. *arXiv*, 2023.
- Xiao, G., Tian, Y., Chen, B., Han, S., and Lewis, M. Efficient streaming language models with attention sinks. In *ICLR*. OpenReview.net, 2024.
- Yang, Z., Qi, P., Zhang, S., Bengio, Y., Cohen, W. W., Salakhutdinov, R., and Manning, C. D. Hotpotqa: A dataset for diverse, explainable multi-hop question answering, 2018. URL <https://arxiv.org/abs/1809.09600>.
- Zellers, R., Holtzman, A., Bisk, Y., Farhadi, A., and Choi, Y. HellaSwag: Can a machine really finish your sentence? In *Proceedings of the 57th Annual Meeting of the Association for Computational Linguistics*, pp. 4791–4800, Florence, Italy, July 2019. Association for Computational Linguistics. doi: 10.18653/v1/P19-1472. URL <https://aclanthology.org/P19-1472>.
- Zhang, H., Ji, X., Chen, Y., Fu, F., Miao, X., Nie, X., Chen, W., and Cui, B. Pqcache: Product quantization-based kvcache for long context llm inference, 2024. URL <https://arxiv.org/abs/2407.12820>.
- Zhang, Z., Sheng, Y., Zhou, T., Chen, T., Zheng, L., Cai, R., Song, Z., Tian, Y., Ré, C., Barrett, C., Wang, Z., and Chen, B. H<sub>2</sub>O: Heavy-hitter oracle for efficient generative inference of large language models, 2023. URL <https://arxiv.org/abs/2306.14048>.
- Zheng, L., Chiang, W.-L., Sheng, Y., Zhuang, S., Wu, Z., Zhuang, Y., Lin, Z., Li, Z., Li, D., Xing, E., et al. Judging llm-as-a-judge with mt-bench and chatbot arena. *Advances in Neural Information Processing Systems*, 36: 46595–46623, 2023.

Table 3: Percent of attention scores required to reach 95% of dense attention performance for different categories of tasks, along with the average entropy of the attention vectors for tokens generated from those tasks.

Task Category	k Required For 95% Performance	Attention Entropy
Needle In A Haystack	0.001%	1.93
Multiple NIAH	0.27%	2.33
Question Answering	0.23%	2.27
Variable Tracking	0.11%	2.11
Word Counting	8.87%	2.68
<b>Correlation coefficient</b>	0.847	

## A. Appendix

### A.1. Distribution of Attention Scores

In general, 1% of the total attention scores are sufficient for providing 95% of the performance of dense attention on Open LLM Leaderboard, AlpacaEval, and RULER. However, within the subtasks for a given benchmark there is variation in this  $k$ -required threshold. This variation is highly correlated with the a measurement we call the *attention entropy*. Attention entropy is calculated by taking the Shannon entropy of a single row of an attention matrix after the softmax transformation is applied, and averaging that over multiple tokens of generation on many different samples of text.

When treating a single, soft-maxed row of an attention matrix as a probability distribution, entropy serves as a good descriptor of how concentrated, or "sparse" it is. The entropy of a maximally concentrated attention distribution is zero, while completely uniform attention scores would have an entropy of the logarithm total scores. Thus low entropy indicates sparse, or concentrated attention. In table 3 we show the attention entropy calculated from the first ten tokens of generation from fifty samples of text in each task category. The attention entropy values in the table have a Pearson correlation coefficient of 0.85 with the  $k$ -required thresholds for 95% performance in those tasks.

In addition to looking at the attention distributions across tasks, we investigate if there are any systematic trends in the attention sparsity across layers of a model. Figure 9) shows the attention entropy for RULER subtasks when plotted by layer, and figure 3 shows the number of scores required to cover 75% of the full attention distribution, with a histogram plotting this value over hundreds of samples of Wikipedia text. Note that in both figures, the first layer clearly stands out as having the least concentrated attention distributions.

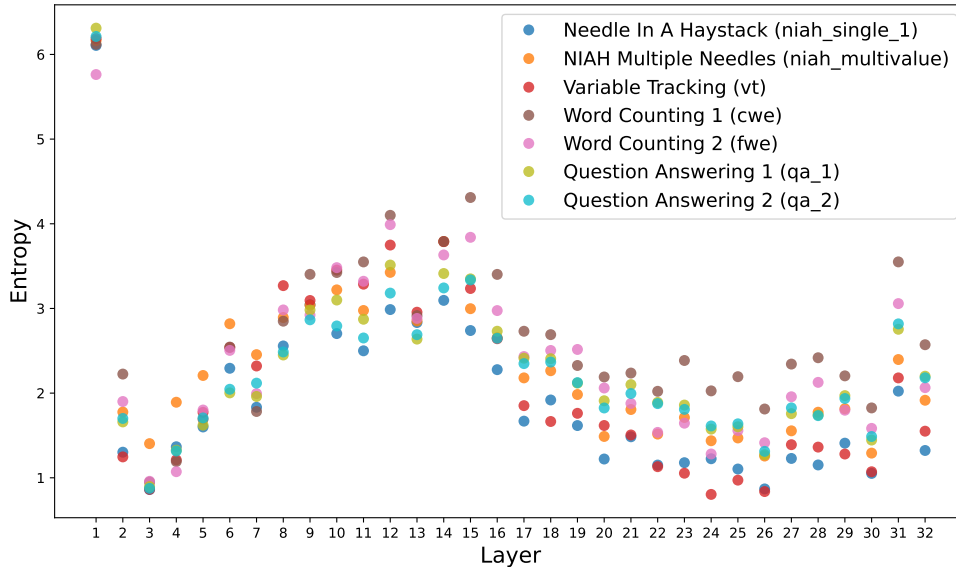


Figure 9: Attention entropy by layer, colored by task category.



Figure 10: All 32 layers are plotted in order, where the top row represents layers 1, 2, 3, and 4 and last row represents layers 29, 30, 31, and 32.



## A.2. Additional RULER and AlpacaEval Results

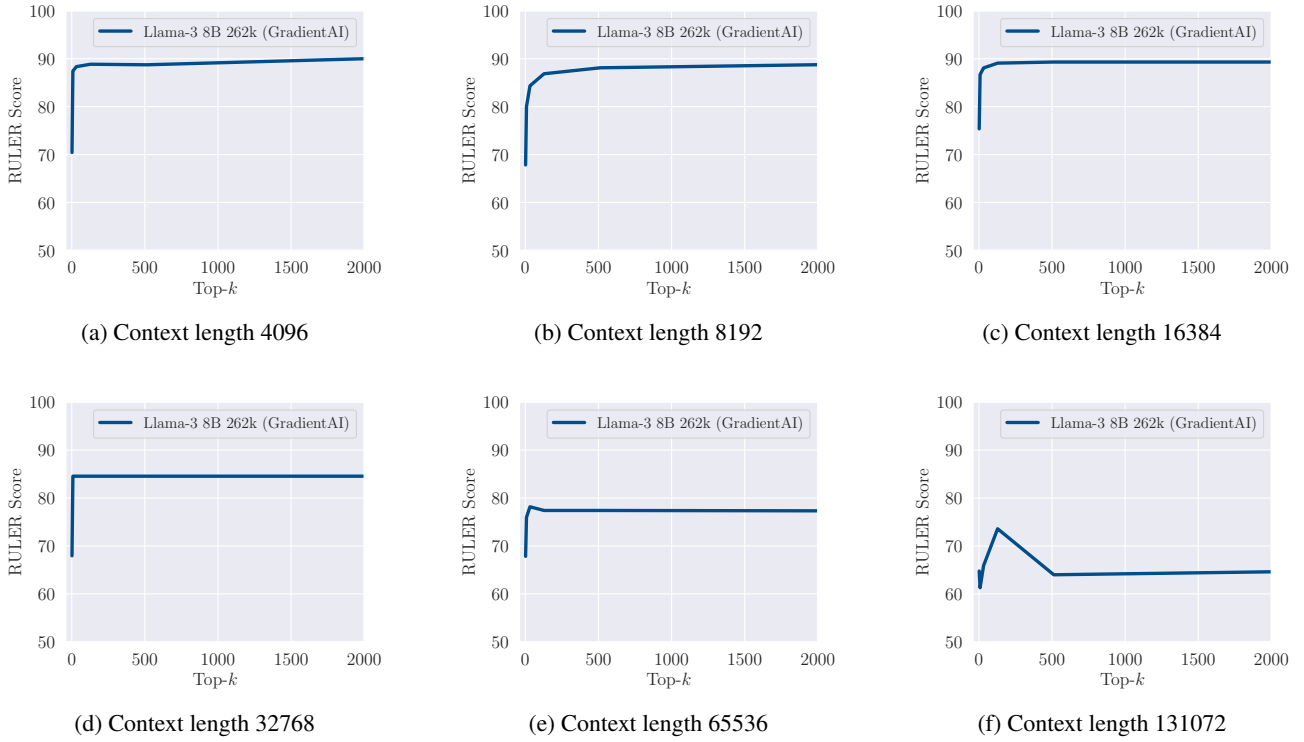


Figure 11: Results for RULER over various context lengths. This shows the same behavior as Open LLM Leaderboard and AlpacaEval where very few attention scores (very low  $k$ ) are sufficient to achieve near dense attention performance.

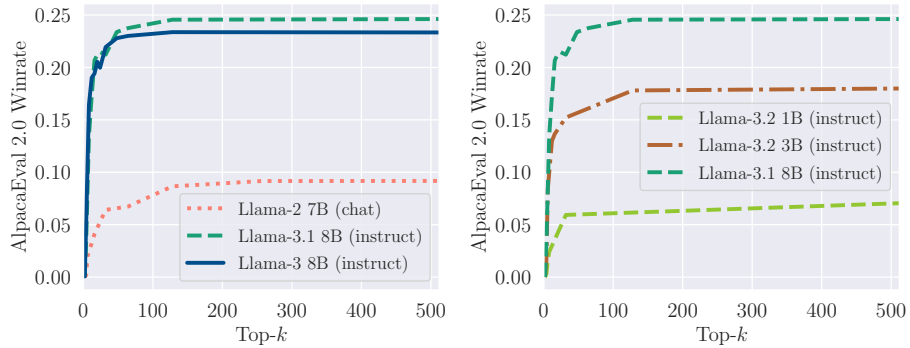


Figure 12: AlpacaEval 2.0 results for various models. Left compares different generations of Llama instruction tuned models. Right investigates how models of different sizes handle small values of  $k$ .